China Geology 7 (2024) 80−90

China Geology

Journal homepage: http://chinageology.cgs.cn
https://www.sciencedirect.com/journal/china-geology

Plume-lithosphere interaction in the Comei Large Igneous Province: Evidence from two types of mafic dykes in Gyangze, south Tibet, China

Ya-ying Wang[a,*], Ling-sen Zeng[a], Li-e Gao[a], Li-long Yan[a], Ling-hao Zhao[b], Jia-hao Gao[c], Ying-long Di[a], Guang-xu Li[a], Yi-hong Tian[a]

[a] *Institute of Geology, Chinese Academy of Geological Sciences, Beijing* 100037, *China*
[b] *National Research Center for Geoanalysis, Chinese Academy of Geological Sciences, Beijing* 100037, *China*
[c] *China Nonferrous Metals (Guilin) Geology and Mining Co., Ltd, Guilin* 541004, *China*

ARTICLE INFO

Article history:
Received 14 December 2022
Received in revised form 14 February 2023
Accepted 28 March 2023
Available online 12 April 2023

Keywords:
OIB type diabase
Comei Large Igneous Province
Weakly enriched diabase
Plume-lithosphere interaction
Nb-Ta-Ti negative anomaly
Kerguelen plume
Geological survey engineering
Tibet Plateau

ABSTRACT

Two suites of mafic dykes, T1193-A and T1194-A, outcrop in Gyangze area, southeast Tibet. They are in the area of Comei LIP and have indistinguishable field occurrences with two other dykes in Gyangze, T0902 dyke with 137.7±1.3 Ma zircon age and T0907 dyke with 142±1.4 Ma zircon age reported by Wang YY et al. (2016), indicating coeval formation time. Taking all the four diabase dykes into consideration, two different types, OIB-type and weak enriched-type, can be summarized. The "OIB-type" samples, including T1193-A and T0907 dykes, show OIB-like geochemical features and have initial Sr-Nd isotopic values similar with most mafic products in Comei Large Igneous Provinces (LIP), suggesting that they represent melts directly generated from the Kerguelen mantle plume. The "weak enriched-type" samples, including T1194-A and T0902 dykes, have REEs and trace element patterns showing within-plate affinity but have obvious Nb-Ta-Ti negative anomalies. They show uniform lower $\varepsilon_{Nd}(t)$ values (−6–−2) and higher $^{87}Sr/^{86}Sr(t)$ values (0.706–0.709) independent of their MgO variation, indicating one enriched mantle source. Considering their closely spatial and temporal relationship with the widespread Comei LIP magmatic products in Tethyan Himalaya, these "weak enriched-type" samples are consistent with mixing of melts from mantle plume and the above ancient Tethyan Himalaya subcontinental lithospheric mantle (SCLM) in different proportions. These weak enriched mafic rocks in Comei LIP form one special rock group and most likely suggest large scale hot mantle plume-continental lithosphere interaction. This process may lead to strong modification of the Tethyan Himalaya lithosphere in the Early Cretaceous.

1. Introduction

Compared with oceanic large igneous provinces (LIP) or oceanic flood basalts, LIPs occurred in continents usually have isotopic and trace element signatures varied in large ranges, such as Deccan Trap (Lightfoot PC et al., 1990) and Emeishan continental flood basalt (Xu YG et al., 2004). These large chemical and isotopic variations require the incorporation of lithospheric components during the magmatic process and witness complex interaction between mantle plume and the above continental lithosphere (Gallagher K and Hawkesworth C, 1992; Xiao YG et al., 2004). Identifying the potential plume-continental lithosphere interaction process in one continental LIP can not only be helpful to understand the activity model of the underlying mantle plume, but also be one good way to reveal the evolution and modification history of the overlying ancient continental lithosphere.

Comei Large Igneous Province (LIP), including mafic intrusions and dike swarms in the Comei-Yamdrok-Gyangze areas from eastern Tethyan Himalaya (Fig. 1), represents the eroded remnants of a LIP associated with the breakup of the eastern Gondwana supercontinent upon the impact of the Kerguelen mantle plume in the Early Cretaceous (Zhu DC et al., 2009; Shi YR et al., 2018; Wang YY et al., 2022; Wu H et al., 2023). In Comei LIP, evidences for the participation of Kerguelen mantle plume include: (1) Early Cretaceous mafic

* Corresponding author: *E-mail address*: yywanggeo@163.com (Ya-ying Wang).

Literary editor: Xi-jie Chen
doi:10.31035/cg2023023
2096-5192/© 2024 China Geology Editorial Office.

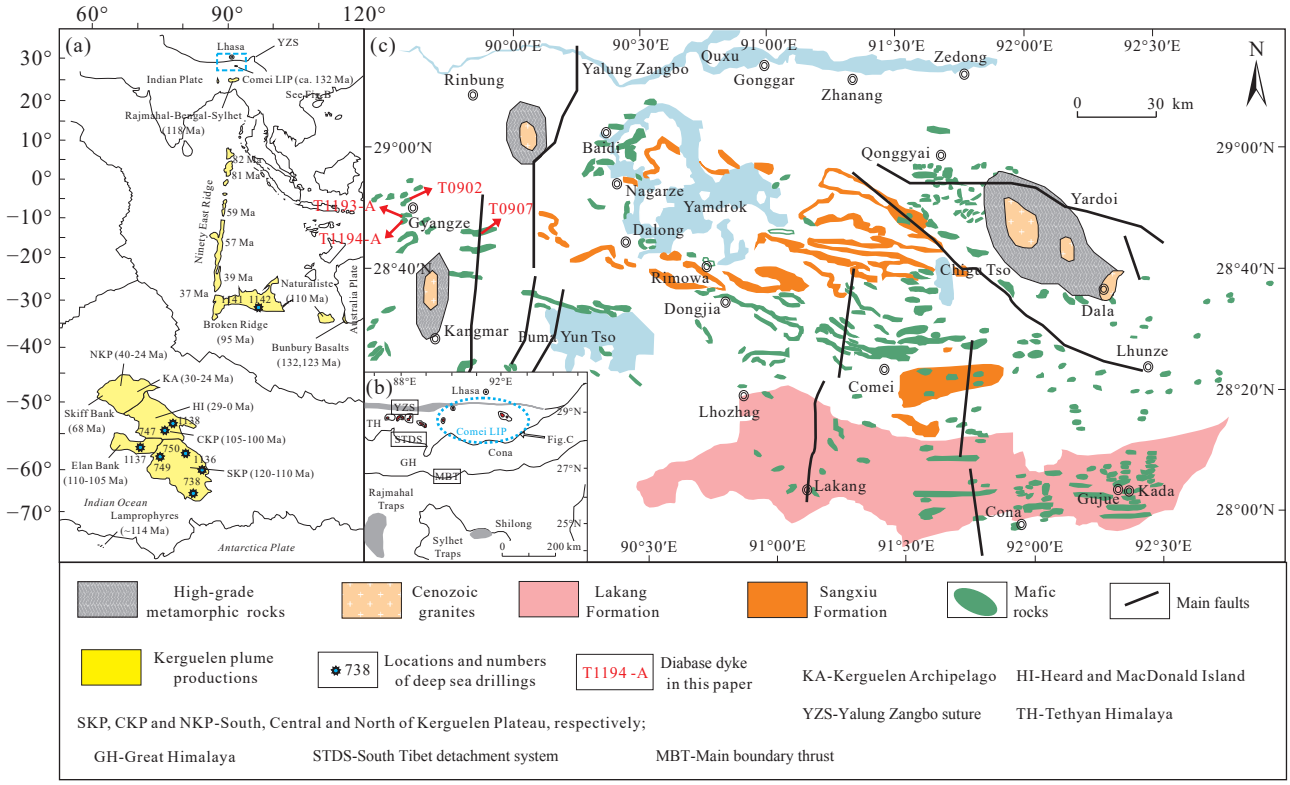

Fig. 1. a–Physiographic map of the Indian Ocean and surrounding continents, showing spatial-temporal locations of the Comei LIP and other products created by the Kerguelen plume (after Zhu DC et al., 2008); b–sketch tectonic map of the east-central Tethyan Himalaya and eastern India showing the present location of the Comei LIP (after Zhu DC et al., 2009); c–simplified geologic map showing spatial extent and distributions of Comei LIP (after Wang YY et al., 2022) and the location of T1193-A and T1194-A dykes. Other samples, T0902 and T0907, in Gyangze are from Wang YY et al. (2016).

dykes widely exposed in the eastern Tethyan Himalaya show OIB-type main and trace element compositions similar with other products from Kerguelen plume (Zhu DC et al., 2008; Wang YY et al., 2016; Zhou Q et al., 2017); (2) Picritic rocks with Early Cretaceous age are reported in Cona area with high mantle potential temperature (T_P >1550°C, Xia Y et al., 2014); (3) Many mafic rocks in Comei LIP have Sr-Nd-Pb-Hf-Os initial isotopic values close to Kerguelen plume (Chen SS et al., 2021); (4) Westward migration of volcaniclastic sedimentation from east Tethyan Himalaya indicates domal surface uplift associated with magmatic upwelling from the underlying mantle plume (Hu XM et al., 2015). However, the large variation of initial Sr-Nd isotopic and trace element compositions of mafic rocks in Comei LIP (Wang YY et al., 2022) suggest complicated interactions among the Kerguelen plume, eastern Gondwana lithosphere and the upwelling asthenosphere. With increasing researches about mafic rocks in Comei LIP published in recent years (Wei YS et al., 2017; Wang YY et al., 2020; Xia Y et al., 2020), the associated activity model of the Kerguelen plume during the formation of the Comei LIP still need to be constrained.

In this contribution, the authors present new whole-rock element concentration and Rb-Sr and Sm-Nd isotope ratio results from two diabase dykes closely outcropped in Gyangze area, south Tibet (Fig.1). First, the authors use these data to determine the petrogenesis of these two dykes. Then, the authors summarize and compare coeval mafic dyke rocks with similar occurrences in Gyangze area (Wang YY et al., 2016). The authors find that these dykes in Gyangze, located in the area defined as Comei LIP, can be classified into two types, OIB-type and weak enriched-type. The former can be produced by partial melting of Kerguelen mantle plume and the latter represents mixing melts from mantle plume and the above enriched subcontinental lithospheric mantle, respectively. These two types of mafic rocks also widely distribute in the other parts of Comei LIP and can be used to constrain the plume-lithosphere interaction process during the formation of Comei LIP.

2. Geology background and sample locations

As part of the Himalaya orogenic belt, Tethyan Himalaya locates between the Yarlung Tsangpo Suture (YTS) to the north and the Greater Himalayan Crystalline Sequence (GHCS) to the south (Fig. 1). The Tethyan Himalayan sedimentary succession represents the deformed remnant in the northern margin of the Indian subcontinent (Liu G and Einsele G, 1994), and the Mesozoic sedimentary rocks in it are well preserved and exposed (Sciunnach D and Garzanti E, 2012). A mass of mafic intrusions and dike swarms intruding into the Jurassic-Cretaceous sedimentary sequences in Comei-Yamdrok-Gyangze areas, eastern Tethyan Himalaya have been grouped into the Comei LIP, including diabase rock beds/walls, gabbro intrusions, and a small amounts of

ultramafic rocks (Fig. 1c; Zhu DC et al., 2009; Xia Y et al., 2014; Liu Z et al., 2015; Wang YY et al., 2016, 2018).

Two diabase dykes in this paper, T1193-A dyke and T1194-A dyke, are located very close to each other in the south of Gyangze town (Fig.1c). Both of them intruded in limestones and shales in the Ridang Formation with approximately E-W trending along the strike and extending for few tens of meters. The Ridang Formation contains slates, calcic siltstone, shales, and limestones, which belongs to Early Jurassic in age (Wan XQ and Liu WC, 2005). Five samples in T1193-A dyke and six samples in T1194-A dyke from center to margin have been collected. Most samples consist of similar mineral assemblages, including clinopyroxenes, plagioclases, and ilmenites with minor apatite and zircons (Fig. 2).

In the authors ' previous work, samples from other two mafic dykes around Gyangze, T0902 dyke with zircon U-Pb age of 137.7 ± 1.3 Ma and T0907 dyke with zircon age of 142.0 ± 1.4 Ma, have been reported by Wang YY et al. (2016). The sample location relationships for the above four mafic dykes are shown in Fig. 1c. All the four dykes around Gyangze town show similar occurrences intruded into the Ridang Formation with near E-W trending, strongly indicating similar formation time. Therefore, the authors view T1193-A and T1194-A samples with similar formation ages during Early Cretaceous, consistent with the period of Comei LIP (Wang YY et al., 2020).

3. Analytical methods

The rocks were crushed and ground in a tungsten carbide shatter box. The resulting whole-rock powders for five samples from T1193-A dyke and 6 samples from T1194-A dyke were prepared for analyses of major and trace elements. Major element compositions were obtained by X-ray fluorescence (XRF), and trace and rare earth element concentrations by inductively coupled plasma mass spectrometry (ICP-MS) at the National Research Center for Geoanalysis, CAGS. Major elements by the XRF method have analytical uncertainties <5%. Trace and REE were separated using cation-exchange techniques before ICP-MS analysis. Analytical uncertainties are estimated at 10% for elements with abundances $<10 \times 10^{-6}$, and about 5% for those $>10 \times 10^{-6}$. Analytical procedures are the same as these described by Wang YY et al. (2018) and analytical results are listed in Table S1.

Whole-rock Rb-Sr and Sm-Nd isotopic analyses for 10 samples in total were performed at University of Science and Technology of China, Hefei, China, following the procedures described in Chen FC et al. (2000, 2007). Whole-rock powders of about 100 mg were weighed and placed in 15 mL Teflon stuffy tanks and were dissolved in a mixture of 2–3 mL purified HF solution and 8–10 drops of purified $HClO_4$ solution. Decomposition of refractory phases was ensured by heating the samples in Teflon stuffy tank at 120°C for about 7 days. After the samples were completely dissolved, the sample solutions were dried on a hotplate at 120°C to make the samples dried, and then heated to 150°C to completely remove the HF and $HClO_4$. 3 mL purified 6N HCl solution was added into the sample tanks twice to clear the inside of the tanks and then dried again. The sample residues were re-dissolved overnight with 1 ml purified 3N HCl solution to prepare for chemical separation and purification.

Sr and light rare earth elements were isolated on quartz columns by conventional ion exchange chromatography with a 5 mL resin bed of Bio Rad AG 50W–X12, 200–400 mesh. Nd was separated from other rare earth elements on quartz columns using 1.7 mL Teflon powder coated with HDEHP, di (2-ethylhexyl) orthophosphoric acid, as the cation exchange medium. All isotopic measurements were done on a Finnigan MAT 262 mass spectrometer. Sr was loaded with a Ta-HF activator on preconditioned W filaments and was measured in single-filament mode. Nd was loaded as phosphate on preconditioned Re filaments and measurements were performed in a Re double filament configuration. The $^{87}Sr/^{86}Sr$ ratios were normalized to $^{86}Sr/^{88}Sr = 0.1194$ and the $^{143}Nd/^{144}Nd$ ratios to $^{146}Nd/^{144}Nd = 0.7219$. Analytical results are listed in Table S2. Initial Sr and Nd isotope compositions are calculated based on about 132 Ma as their assumed crystallization ages.

4. Data results

In terms of whole-rock major element compositions

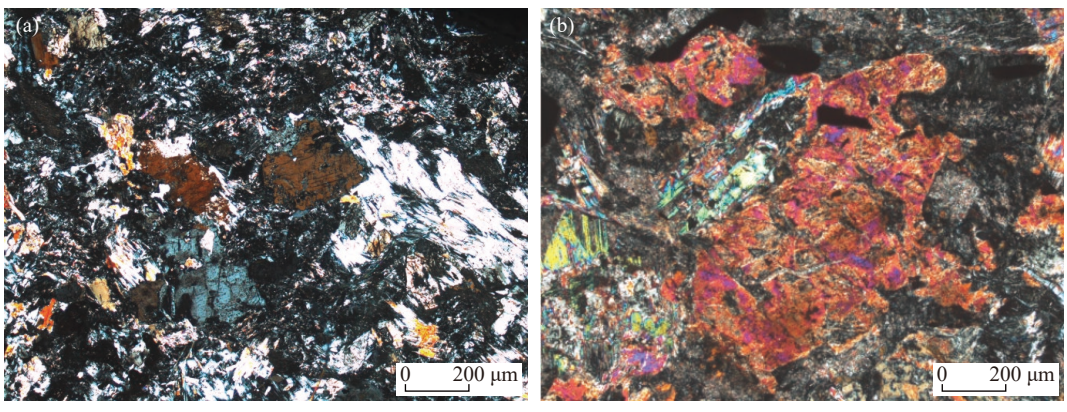

Fig. 2. Microphotographs of diabase dyke samples in Gyangze (a) T1193-A and (b) T1194-A.

(Table S1), 5 samples from T1193-A dyke contain constant SiO_2 (45.3%–47.5%), MgO (5.1%–5.4%), TFeO (total Fe as FeO, 9.4%–9.9%), CaO (5.5%–6.5%), Al_2O_3 (12.1%–12.7%), TiO_2 (3.5%–3.9%) and Na_2O (2.4%–3.2%) contents and low contents of P_2O_5 (0.4%) and K_2O (0.1%–0.2%). The LOI (loss on ignition) values vary in range from 9.3% to 12.4%, suggesting large degree of alteration. 6 samples from T1194-A dyke contain constant SiO_2 (52.3%–53.2%) and MgO (5.1%–8.7%) contents, varied contents of TFeO (8.4%–9.6%), CaO (6.6%–8.6%), Al_2O_3 (11.9%–15.0%), TiO_2 (2.0%–2.4%) and Na_2O (1.7%–2.5%), and low P_2O_5 (0.3%) and K_2O (1.3%–2.2%) contents. The low LOI values vary in range from 1.8 % to 3.3 %, suggesting limited degree of alteration. In addition, concentrations of compatible elements from T1194-A dyke samples also show large variation ranges with 152×10^{-6}–812×10^{-6} Cr, 32×10^{-6}–43×10^{-6} Co, 39×10^{-6}–94×10^{-6} Ni and 223×10^{-6}–257×10^{-6} V.

All dyke samples in Gyangze area belong to sub-alkaline series in SiO_2 versus Na_2O+K_2O diagram (Fig. 3a) and plot around andesite/basaltic andesite and basalt fields on the Nb/Y versus Zr/TiO_2 diagram (Fig. 3b). Taking all the four coeval mafic dykes in Gyangze area into consideration, samples from T1193-A and T1194-A dykes show similar MgO contents with T0907 samples (4.6%–5.2%), suggesting similar magma evolution degree (Fig. 4a). Whereas T0902 samples have the highest MgO values (10.3%–15.0%), indicating that they represent relatively primitive magma components (Fig. 4a). Samples from T1193-A dyke have major element compositions almost the same with T0907 samples in the variation diagrams of selected major oxides versus MgO (Fig. 4). However, T1194-A samples show much lower TiO_2, TFeO, P_2O_5 and Na_2O contents and higher CaO and K_2O contents in Fig. 4.

In terms of whole-rock trace element compositions (Table S1), concentrations of REEs in T1193-A samples and T1194-A samples are moderate with ∑REE ranging from 169×10^{-6} to 183×10^{-6} and 168×10^{-6} to 179×10^{-6}, respectively, varying between T0902 dyke (81×10^{-6}–103×10^{-6}) and T0907 dyke (196×10^{-6}–234×10^{-6}). All samples in Gyangze area show enrichment of LREEs than HREEs (Figs. 5a and c), similar to typical OIB pattern (Sun SS and McDonough WF, 1989). Both T1193-A samples and T1194-A samples are characterized by high degree of differentiation between LREEs and HREEs (Figs. 5a and c) with $(La/Yb)_N$ (N-normalized to chondrites) from 6.37 to 6.88 and 6.94 to 7.44, respectively, and relatively steep heavy-rare-earth element patterns on a primitive mantle–normalized spider diagram (Figs. 5b and d). The Eu anomies are not obvious with Eu/Eu* varying from 0.92 to 1.02 of T1193-A dyke and 0.84 to 0.94 for T1194-A dyke. However, compared with typical OIB rocks, T1193-A samples show low contents and irregular variations of LILEs (Rb and Ba) and obviously negative K and Sr anomalies in Fig. 5b. These are most likely due to their large degree of post-magmatic alteration, consistent with their high LOI values. Without consideration the irregular LILEs, distribution pattern of other immobile trace elements (HFSEs) for T1193-A dyke in Fig. 5b is almost same with T0907 dyke in the east (Fig. 1c), which is nearly identical with typical OIB in Fig. 5b. On the other hand, compared with typical OIB rocks, T1194-A samples show irregular variations of LILEs (Rb, Ba, Th, U and K) and obviously positive Pb and negative Nb-Ta-P-Ti anomalies in Fig. 5d. This trace element distribution pattern is consistent with T0902 dyke in the north (Fig. 1c).

Isotopic Sr and Nd data for 10 whole rock samples from T1193-A and T1194-A dykes are listed in Table S2. The initial isotopic compositions of analyzed samples are graphically presented on the $\varepsilon_{Nd}(t)$ versus $^{87}Sr/^{86}Sr(t)$ diagram (Fig. 9a). Samples from T1193-A dyke show similar initial Sr isotopic compositions ($^{87}Sr/^{86}Sr(t)$ =0.706594–0.707786) and high $\varepsilon_{Nd}(t)$ values (+3.30–+6.47). To comparison, samples from T1194-A dyke show relatively higher $^{87}Sr/^{86}Sr(t)$ values from 0.707845 to 0.708573 and much lower $\varepsilon_{Nd}(t)$ values from −4.28 to −2.04.

TiO_2 content and Ti/Y ratio have been viewed as important parameters to reflect the geochemical characteristics of mafic rocks (Xiao YG et al., 2004). Consistent with TiO_2 content variations (3.5%–3.9% of T1193-A dyke and 2.0%–2.4% of T1194-A dyke), Ti/Y ratios vary from 630 to 697 of T1193-A samples and from 378 to

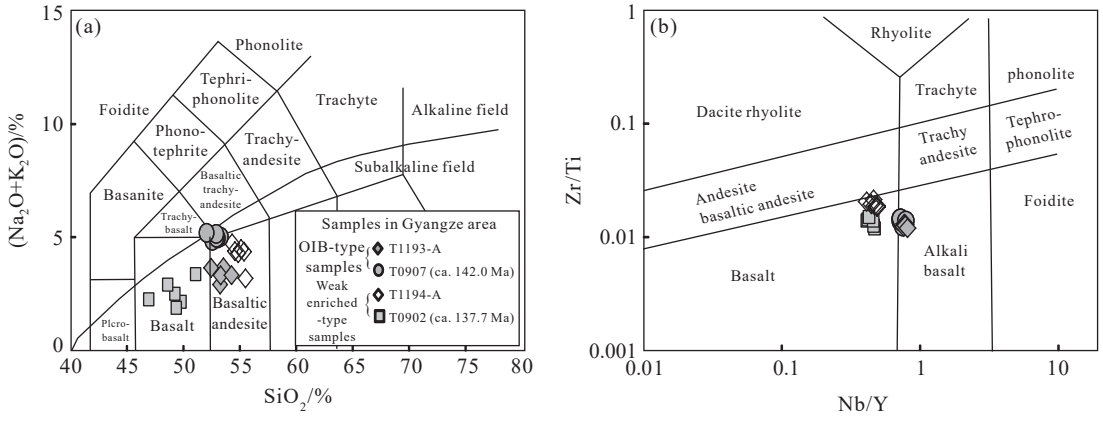

Fig. 3. Classification of diabase dyke samples in Gyangze. a–IUGS-recommended TAS diagram of Le Bas MJ and Streckeisen AL (1991); b–an immobile element-based TAS proxy diagram (after Floyd PA and Winchester JA, 1975). T0907 and T0902 samples are from Wang YY et al., (2016).

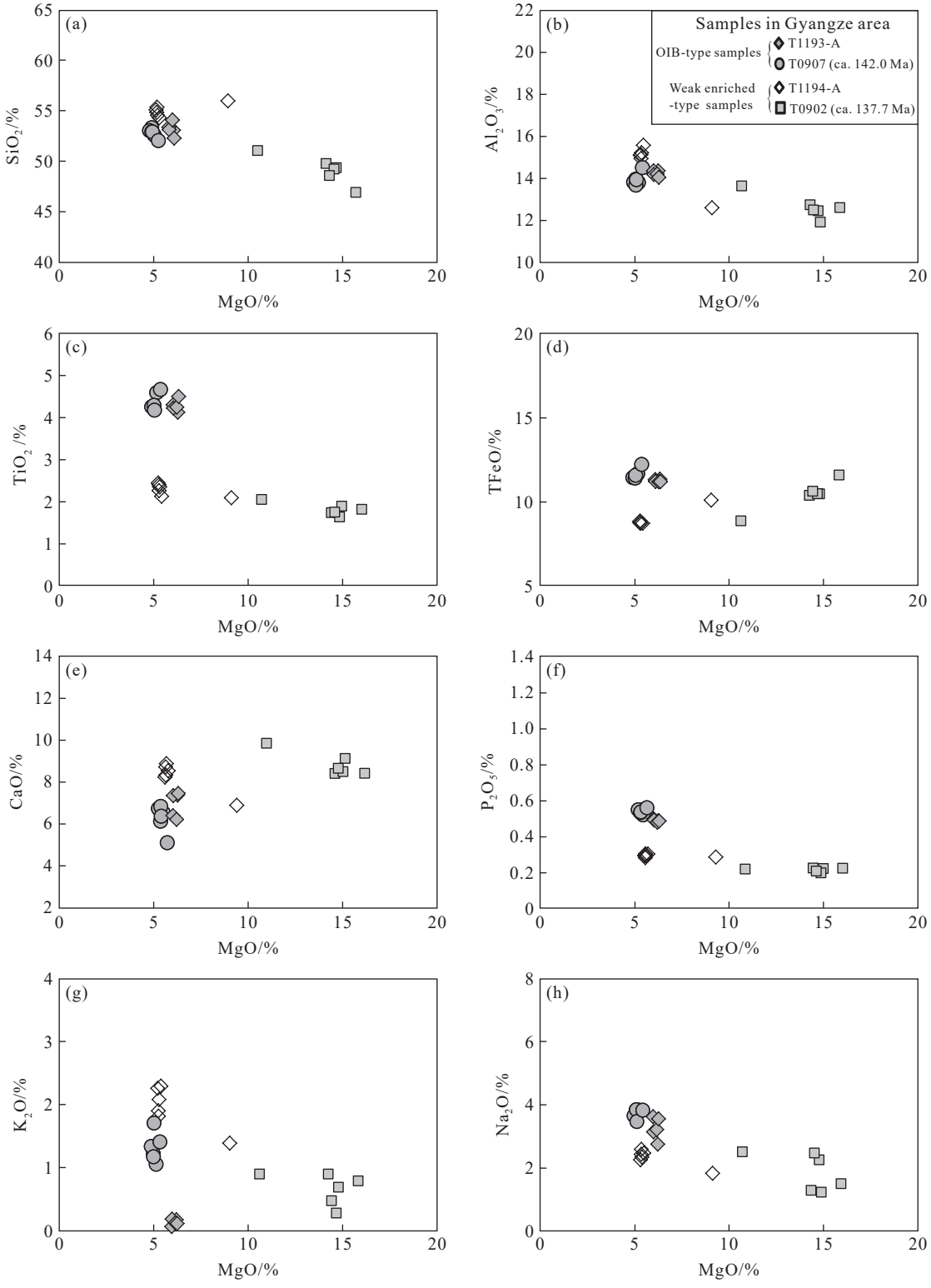

Fig. 4. Variation diagrams of major oxides (%) versus MgO (%) of Gyangze samples in Comei LIP. T0907 and T0902 samples are from Wang YY et al., (2016). All major oxide percentages were recalculated after removing their LOI values.

446 for T1194-A samples (Table 1). The Ce/Pb (19–30) and Nb/U (38–45) ratios from T1193-A samples are similar with T0907 dyke, but these ratios for T1194-A samples (Ce/Pb: 10–16 and Nb/U: 9–12) are more consistent with T0902 dyke (Fig. 10 and Table 1).

To summarize, it can be found that these Early Cretaceous dykes in Gyangze area show varied geochemistry compositions (Table 1). In detail, "OIB-type" rocks, the T1193-A dyke and T0907 dyke, have trace element features and initial Sr-Nd isotopic values almost identical with typical OIB. Whereas, "weak enriched-type" rocks, the T1194-A and T0902 dykes, show similar within-plate features but with obvious negative Nb-Ta-Ti anomaly and enriched Sr-Nd initial isotopic ratios. These different geochemical features

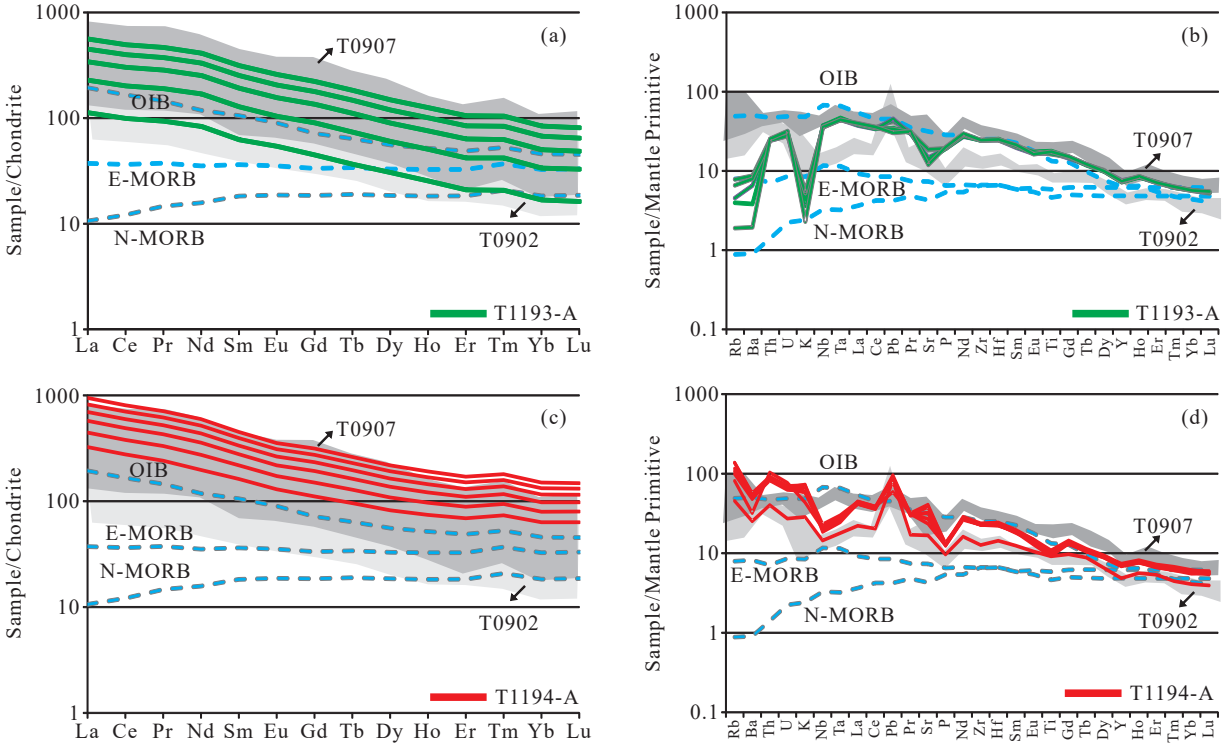

Fig. 5. (a and c) Rare earth element distribution diagrams and (b and d) trace element distribution diagrams. The shaded areas are coeval Gyangze samples from Wang YY et al. (2016). Data of chondrite, primitive mantle, OIB, E-MORB and N-MORB are from Sun SS and McDonough WF (1989).

Table 1. Contrasts of some element ratios and isotopic values of "OIB-type" and "weak enriched-type" diabase rocks in Gyangze area, South Tibet.

	$\varepsilon_{Nd}(t)$	$^{87}Sr/^{86}Sr(t)$	Nb/La	Ce/Pb	Nb/U	Nd/Pb	Ti/Y
OIB-type	+3.3–+6.5	0.7054–0.7079	0.84–1.04	16–33	26–45	10–21	578–710
Weak enriched-type	−1.6—−4.3	0.7068–0.7086	0.45–0.68	4–16	9–18	2–9	378–555

suggest that they may be derived from two different mantle sources during the formation of Comei LIP.

5. Discussion

Above four Gyangze diabase dykes in the area of Comei LIP in southeast Tethyan Himalaya (Fig. 1c), share indistinguishable field occurrences that they all intrude into the Jurassic to Early Cretaceous formation, extending in east-west for several hundred meters. Importantly, OIB-type and "weak enriched" type rocks in general located closely to each other with very similar crystalline ages, such as T0902 and T0907 dykes in Gyangze area (Wang YY et al., 2016). Their formation period (about 140–130 Ma) is also contemporaneous with the regional mafic rocks that have been grouped into the Early Cretaceous Comei LIP (Fig. 1; Wang YY et al., 2022). The huge amount of heat supplied by Kerguelen mantle plume was necessary for the large volumes of mafic dykes emplaced in the southeast Tethyan Himalaya (Zhu DC et al., 2009). So this closely co-occurrence field relationship implies that both of them must have been influenced by the Kerguelen mantle plume. Their different geochemistry features most likely result from the potential plume-lithosphere interaction process when the large Kerguelen mantle plume head arrival and heat above Tethyan Himalayan lithosphere.

5.1. "Mantle plume" source of "OIB-type" rocks

In Comei LIP, most mafic products have typical OIB-type geochemical features (Zhu DC et al., 2008; Wang YY et al., 2022). They are dominant diabase dikes and basaltic lavas, characterized by OIB-type REE and trace element patterns (Fig. 6), absence of Nb-Ta anomalies, roughly chondritic Nb/La values from 0.76 to 1.11 (Fig. 9b) with $\varepsilon_{Nd}(t)$ values from +0.5 to +5.0 and $^{87}Sr/^{86}Sr(t)$ values from 0.704 to 0.708 (Fig. 9a, after Wang YY et al., 2022). This geochemical feature is in the range of other magmatic products from the Kerguelen mantle plume (shade areas in Fig. 9) and similar to many OIBs worldwide as summarized by White WM (2015). These OIB-type magmatic rocks are widely distributed throughout the Comei LIP, including the Cona, Comei, Rimowa in the east, and Gyangze areas in the west (Fig. 1), which most likely represent melts directly generated from the head of the Kerguelen mantle plume and are summarized as "OIB-type" end member samples in Comei LIP by Wang YY et al., 2022.

Both T1193-A and T0907 diabase dykes in Gyangze area

with typical OIB features keep consistent with above most mafic products summarized in Comei LIP (Wang YY et al., 2022). They show within-plate properties in the Zr versus Zr/Y diagram (Fig. 6a) and plot in OIB field on the Ti/1000 versus V diagram with Ti/V ratios around 70 (Fig. 6b; Shervais JW, 2022). Proxy Th–Nb (Pearce JA, 2008) and Nb–Zr (Fitton JG et al., 1997) are two important geochemical proxies for the identification and classification of mafic basalts that within-plate basalts lie in a diagonal parallel tight MORB–OIB array and basalts erupted at subduction zones are commonly displaced oblique to the array in Fig. 7. Both T1193-A and T0907 dyke samples plot into the OIB area in the MORB-OIB array in Fig. 7 and show similar plotting positions with the "most mafic products in Comei LIP" as shaded areas in Fig. 7. The Nb/U, Ce/Pb and Nd/Pb ratios are uniform in both MORBs and OIBs, distinct from island arc basalts (IAB) with a "crustal" signature (Hofmann AW et al., 1986). The contamination sensitive ratios Nd/Pb (11–19) and Nb/U (38–45) of T1193-A samples also lie close to OIB area regardless of their MgO variation in Fig. 8a–b. All these within-plate features indicate that they contain less "crustal" or "subduction" components not only in their mantle source but also during magma ascent through the crust. In addition, T1193-A and T0907 samples have similar high initial Nd isotopic ratios ($\varepsilon_{Nd}(t)$:+3.2–+6.4) and low initial Sr isotopic ratios ($^{87}Sr/^{86}Sr(t)$: 0.705–0.708, Fig. 9a) as well as relatively high Nb/La ratios (0.8–1.1, Fig. 9b). These isotopic values show the same variations with OIB-type rocks in Comei LIP in Fig. 9. Combined the within-plate trace element features with "OIB-like" initial Sr-Nd isotopic values, it can be concluded that both T1193-A and T0907 diabase dykes in Gyangze represent partial melts directly derived from the Kerguelen mantle plume.

5.2. "Mixing" source of "weak enriched-type" rocks

Compared with above OIB-like T1193-A and T0907 dykes, the T1194-A and T0902 dykes have unique geochemical features. Different from typical OIBs, they are featured by obvious negative Nb-Ta-Ti anomalies in Fig. 5d, and plot outside the diagonal MORB–OIB array in Fig. 7 toward continental crust field. Both T1194-A and T0902 samples with lower $\varepsilon_{Nd}(t)$ values and higher $^{87}Sr/^{86}Sr(t)$ values, plot outside the OIB-type area in Comei LIP and locate in the lower part in Fig. 9a, suggesting different source components. In addition, their contamination sensitive ratios, Nd/Pb (5.43–8.73) and Nb/U (9–12), also lie into area between OIB and continental crust (Figs. 8a,b), indicating obvious "crustal" signature.

These plotting trends (Figs. 7–9) demonstrate that weak

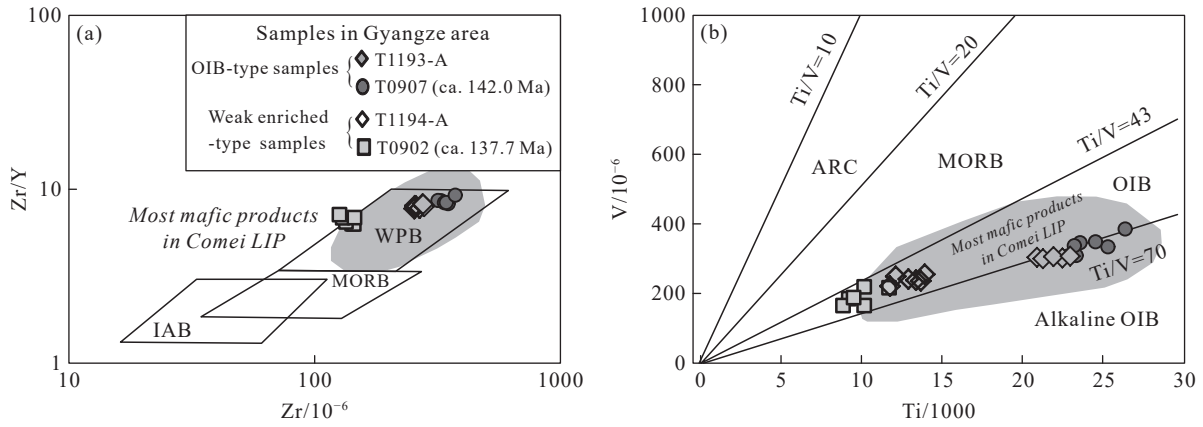

Fig. 6. Tectonic environment discrimination diagram of diabase samples from Gyangze. (a) Zr–Zr/Y diagram (Pearce JA, 1982), WPB: within-plate basalt, MORB: mid-ocean ridge basalt, IAB: island arc basalt and (b) Ti/1000 -V linear plot (Shervais JW, 2022). The shaded areas are "most mafic products in Comei LIP" from OIB-end member samples (Wang YY et al., 2022).

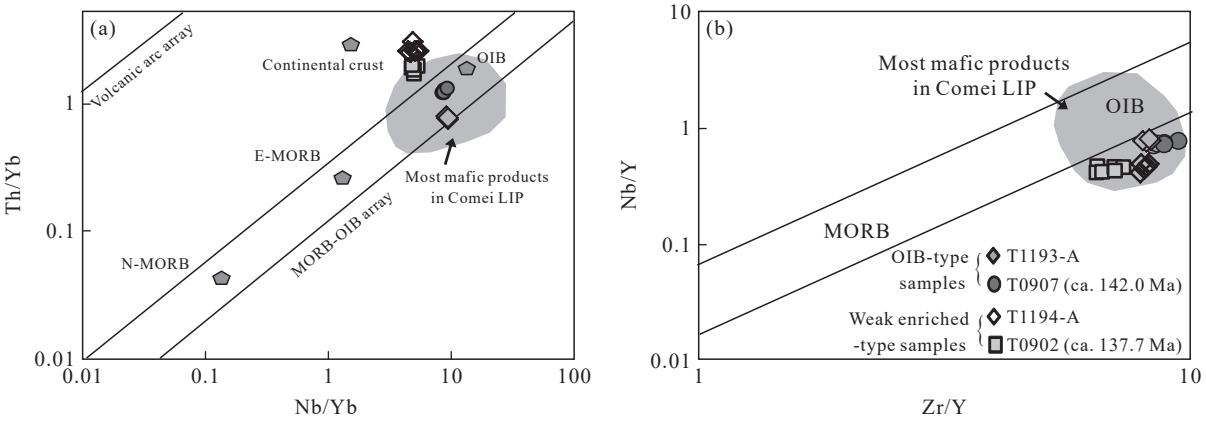

Fig. 7. a–Nb/Yb-Th/Yb (after Pearce JA, 2008); b–Zr/Y-Nb/Y (after Fitton JG et al., 1997) diagrams of diabase samples in Gyangze. The shaded areas are "most mafic products in Comei LIP" from OIB-end member samples (after Wang YY et al., 2022).

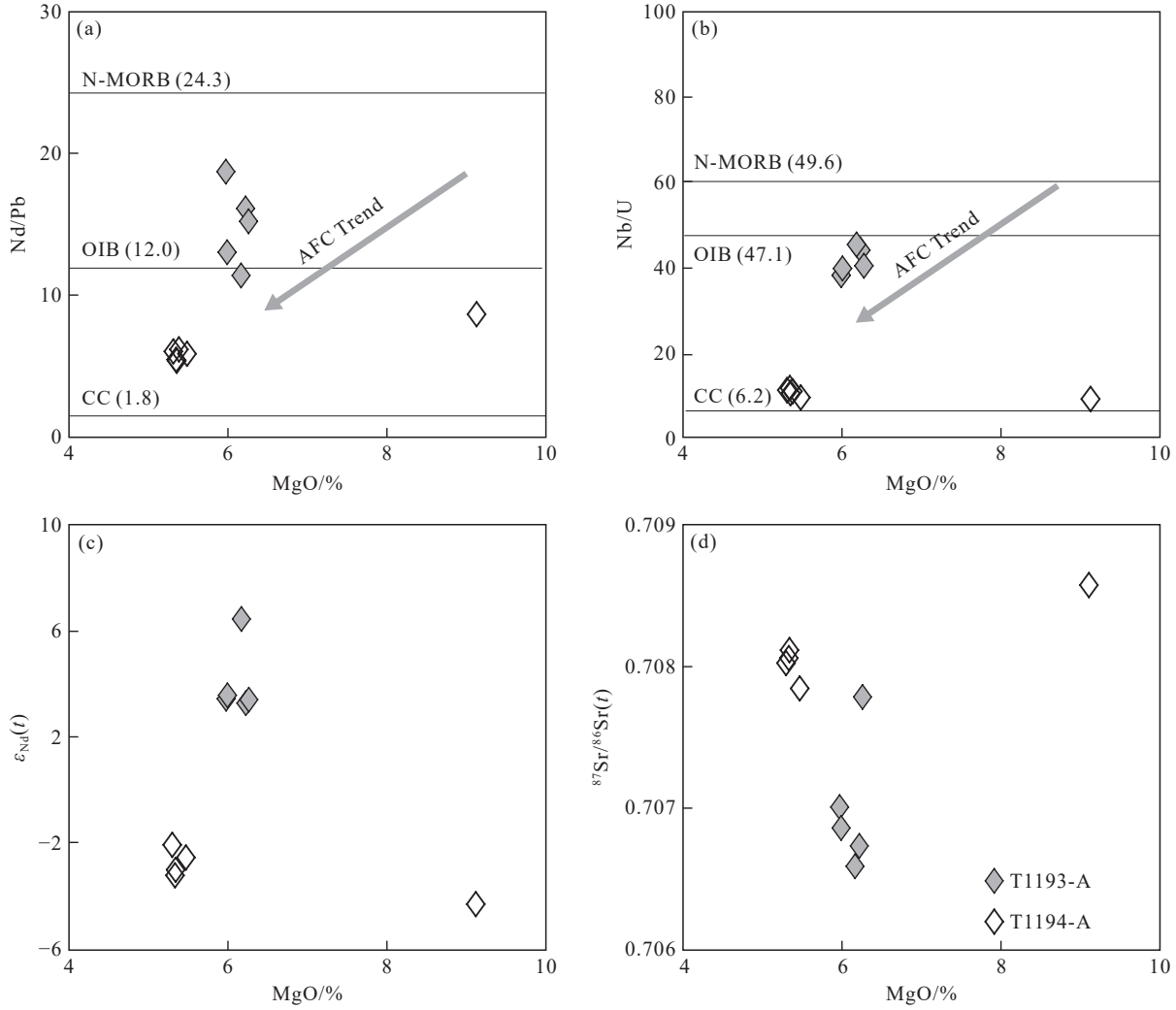

Fig. 8. Plots of (a) Nd/Pb *vs.* MgO, (b) Nb/U *vs.* MgO, (c) $\varepsilon_{Nd}(t)$ *vs.* MgO, and (d) $^{87}Sr/^{86}Sr(t)$ *vs.* MgO of Gyangze samples. The data of OIB, N-MORB, and CC (continental crust) are after Sun SS and McDonough WF (1989) and Rudnick RL and Gao S (2003), respectively. Results show that these diagnostic values sensitive to crustal contamination are nearly uniform within T1194-A samples, independent of MgO variation and do not show AFC trend.

enriched rocks in Gyangze most likely have one hybrid source, which may be produced from AFC (assimilation and fractional crystallization) process during magma ascent through the crust (Lassiter JC and Depaolo DJ, 1997). However, their Nd/Pb, Nb/U ratios and $\varepsilon_{Nd}(t)$ values of T1194-A samples do not decrease with the drop of MgO values (Fig. 8), suggesting limited crustal contamination during magma ascent and that their negative Nb and Ta anomalies are likely inherited from the mantle source. Recently, middle Miocene (about 13 Ma) lamprophyre dike intruded into the Tethyan Himalaya sedimentary was reported (Liu ZC et al., 2020) with enriched initial Sr-Nd isotopic values (Fig. 9), indicating one ancient enriched subcontinental lithospheric mantle (SCLM) in Tethyan Himalaya. Therefore, it is most likely that "crustal" signature in these weak enriched mafic rocks in Comei LIP was inherited from this enriched SCLM.

Nb/U and Ce/Pb ratios can be used to distinguish crustal signature from mantle-derived magma (Hofmann AW et al., 1986). To constrain the mantle source of "weak enriched-type" rocks in detail, the authors use the middle Miocene (about 13 Ma) lamprophyre dike to represent the ancient SCLM in Tethyan Himalaya (Liu ZC et al., 2020), and the OIB-type mafic rocks in Comei LIP to represent Kerguelen mantle plume. In the Nb/U-Nb/La and Ce/Pb-Nb/La correlation figures (Fig. 10), OIB-type mafic rocks in Comei LIP lie into the ranges of global average oceanic basalts, consistent with melting directly from the mantle plume head. At the same time, the weak enriched rocks show large variations spreading between OIB and SCLM fields (Fig. 10), precluding the possibility that they were solely derived from the above enriched SCLM. These positive correlations between Nb/U and Ce/Pb ratios with Nb/La ratios are consistent with melt mixing from mantle plume and SCLM in different proportions to form the "weak enriched-type" rocks (Fig. 10). These middle positions of T1194-A and T0902 samples between SCLM filed and mantle plume field are shown again in the $\varepsilon_{Nd}(t)$ versus Nb/La diagram in Fig. 9b. Therefore, all these evidences suggest that "weak enriched-type" rocks in Comei LIP have "mixing" mantle source with melts derived from both mantle plume and the above enriched SCLM (Wang YY et al., 2018).

5.3. The plume-lithosphere interaction in Comei LIP

Collectively, OIB-type and "weak enriched-type" rocks show similar spatial and temporal distribution in the southeast Tethyan Himalaya with indistinguishable field outcrops (Fig. 1c). These coincidences strongly indicate that they all result from the initial activities of Kerguelen mantle plume in the Early Cretaceous. However, their featured geochemical compositions suggest totally different mantle sources involving large scale plume-lithosphere interaction process. The deep process during the formation of these two magmatic types in Comei LIP can be depicted as followed (Fig. 11): In the beginning, decompression melting of abnormally hot mantle brought to the base of the lithosphere by Kerguelen plume generated the large volumes of the widely distributed OIB-type rocks since about 140 Ma. The above ancient SCLM with enrichment or subduction signature was heated and melting by the underlying Kerguelen plume. Mixing of SCLM-derived melts and plume-derived melts in different proportions formed the weak enriched rocks during almost the same period.

Similar with the "weak enriched-type" rocks in Gyangze, mafic intrusion with negative Nb-Ta-Ti anomaly and ca. 132 Ma zircon U-Pb age has also been reported in Dala area from the east part of Comei LIP (Wang YY et al., 2018). To summarize, these weak enriched rocks locate widely from east to west in Comei LIP. Their "mixing" source features suggest widespread plume-SCLM interaction during the formation of Comei LIP. This process with large influence area strongly indicate that the ancient SCLM in Tethyan Himalaya had experienced significant modification by the strong Kerguelen mantle plume, which may lead to the breakup of east Gondwanaland in the Early Cretaceous (Storey BC et al., 1995).

6. Conclusions

(i) Two types of mafic dykes outcrops in Gyangze area, southeast Tibet. They share the same field occurrences intruded into the Ridang Formation with near E-W trending, but show different geochemistry features. The T1193-A dyke

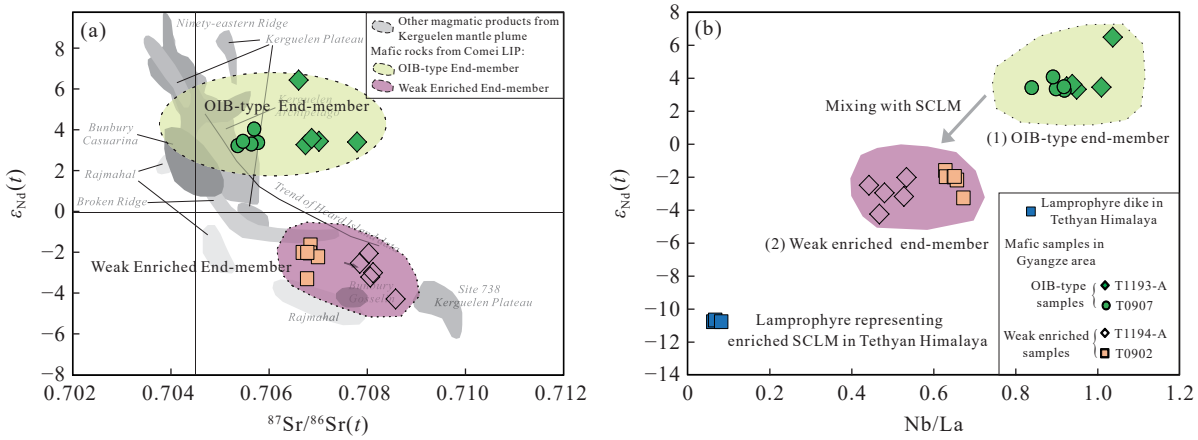

Fig. 9. a–$^{87}Sr/^{86}Sr(t)$ *vs.* $\varepsilon_{Nd}(t)$ diagram and b–Nb/La vs. $\varepsilon_{Nd}(t)$ diagram of diabase samples in Gyangze. *Note*: The shaded areas are basalts related with the Kerguelen plume and different mantel source of mafic products in Comei LIP (after Wang YY et al., 2022). The middle Miocene (about 13 Ma) lamprophyre dike intruded the Tethyan Himalaya sedimentary representing the ancient SCLM in Tethyan Himalaya is from Liu ZC et al., 2020.

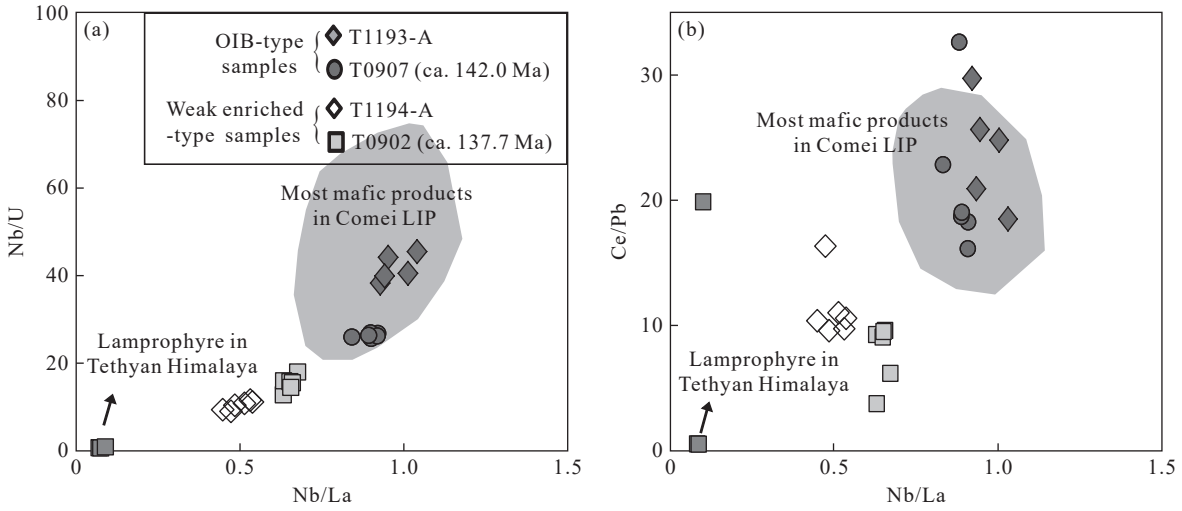

Fig. 10. a–Nb/U-Nb/La plot; b–Ce/Pb-Nb/La plots of diabase samples in Gyangze. The shaded areas are "most mafic products in Comei LIP" from OIB-end member samples (after Wang YY et al., 2022).

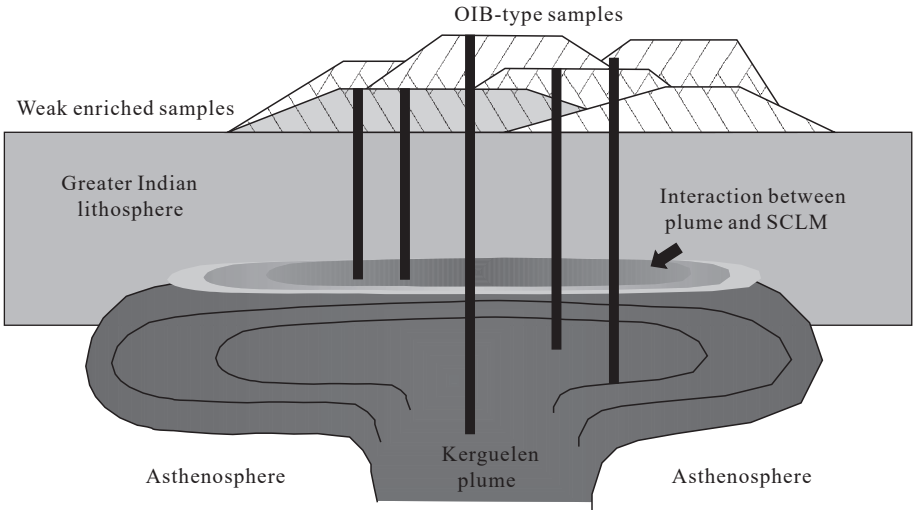

Fig. 11. A proposed model of formation of OIB-type and weak enriched rocks in Comei LIP. Notes: The mantle plume ascends and arrives at the base of Greater Indian lithosphere. The plume head undergoes partial melting of the relatively primitive part of the plume and these melts intruded into the upper crust to form the OIB-type rocks in Comei LIP. Interaction and mixing between melts from mantle plume and melts from the above SCLM formed the weak enriched rocks in Comei LIP. See text for details.

have similar geochemistry features with T0907 dyke formed at 142.0±1.4 Ma (Zircon U-Pb age in Wang YY et al., 2016). They show classical OIB-type trace element features with initial Sr-Nd isotopic values similar with most mafic products in Comei LIP (Fig. 9a), suggesting that both T0907 dyke and T1193-A dyke represent melts directly generated from the head of the Kerguelen mantle plume. The T1194-A mafic dyke show similar geochemical features with T0902 mafic dyke in Gyangze (137.7±1.3 Ma, zircon U-Pb age in Wang YY et al., 2016). They show within-plate affinity but obvious Nb-Ta-Ti negative anomalies and have lower $\varepsilon_{Nd}(t)$ values (−6–−2) and higher $^{87}Sr/^{86}Sr(t)$ values (0.706–0.709), distinct from most mafic products in Comei LIP. Their diagnose trace element ratios (Nb/La, Ce/Pb and Nb/U) plot in the middle position between OIB and SCLM in Tethyan Himalaya, most likely indicating that they represent mixing melts from mantle plume and the above SCLM in different proportions.

(ii) These weak enriched mafic rocks form one special rock group in Comei LIP. Petrogenesis of these weak enriched mafic rocks in Comei LIP suggest large scale hot mantle plume–continental lithosphere interaction. This process may lead to strong modification of the above continental lithosphere in the Early Cretaceous.

CRediT authorship contribution statement

Ya-ying Wang and Ling-sen Zeng conceived of the presented idea and contributed to the final manuscript. All authors carried out the field work and discussed the results.

Declaration of competing interest

The authors declare no conflicts of interest.

Acknowledgment

This study was supported by National Science Foundation of China (42102059 and 92055202), the China Geological Survey (DD20221817 and DD20190057), the basic scientific research funding in CAGS (J2204), and the Second Tibetan Plateau Scientific Expedition and Research (2019QZKK0702). Dr. Zeng Yun-chuan and Dr. Guo Chun-li are thanked for their constructive reviews. Editors Hao Zi-guo and Chen Xi-jie are thanked for carefully handling this paper.

Supplementary dataset

Supplementary data (Tables. S1–S2) to this article can be found online at doi: 10.31035/cg2023023.

References

Chen FK, Hegner E, Todt W. 2000. Zircon ages, Nd isotopic and chemical compositions of orthogneisses from the Black Forest, Germany - evidence for a Cambrian magmatic arc. International Journal of Earth Sciences, 88(2000), 791–802. doi: 10.1007/S00 5310050306.

Chen FK, Li XH, Wang XL, Li QL, Siebel W. 2007. Zircon age and Nd-Hf isotopic composition of the Yunnan Tethyan belt, southwestern China. International Journal of Earth Sciences, 96(2007), 1179–1194. doi: 10.1007/s00531-006-0146-y.

Chen SS, Fan WM, Shi RD, Xu JF, Liu YM. 2021. The Tethyan Himalaya Igneous Province: Early Melting Products of the Kerguelen Mantle Plume. Journal of Petrology, 62(1), 1–22.

Fitton JG, Saunders AD, Norry MJ, Hardarson BS, Taylor RN. 1997. Thermal and chemical structure of the Iceland plume. Earth and Planetary Science Letters, 153, 197–208. doi: 10.1016/S0012-821X(97)00170-2.

Floyd PA, Winchester JA. 1975. Magma type and tectonic setting discrimination using immobile elements. Earth and Planetary Science Letters, 27, 211–218. doi: 10.1016/0012-821x(75)90031-x.

Gallagher K, Hawkesworth C. 1992. Dehydration melting and the generation of continental flood basalts. Nature, 358, 57–59. doi: 10.1038/358057a0.

Hofmann AW, Jochum KP, Seufert M, White WM. 1986. Nb and Pb in oceanic basalts: New constraints on mantle evolution. Earth and Planetary Science Letters, 79, 33–45. doi: 10.1016/0012-821X(86)

90038-5.

Hu XM, Garzanti E, An W. 2015. Provenance and drainage system of the Early Cretaceous volcanic detritus in the Himalaya as constrained by detrital zircon geochronology. Journal of Palaeogeography, 4(1), 85–98. doi: 10.3724/SP.J.1261.2015.00069.

Lassiter JC, Depaolo DJ. 1997. Plume/Lithosphere Interaction in the Generation of Continental and Oceanic Flood Basalts: Chemical and Isotopic Constraint. In: Mahoney, J. J. and Coffin, M. F. (eds.), Large Igneous Provinces: Continental, Oceanic, and Planetary Flood Volcanism. Geophysical Monograph Series, 100, 335–355.

Le Bas MJ, Streckeisen AL. 1991. The IUGS systematics of igneous rocks. Journal of the Geological Society of London, 148, 825–833. doi: 10.1144/gsjgs.148.5.0825.

Liu G, Einsele G. 1994. Sedimentary history of the Tethyan basin in the Tibetan Himalayas. Geol Rundsch 83, 32–61. doi: 10.1007/bf00 211893.

Liu Z, Zhou Q, Lai Y, Qing CS, Li YX, Wu JY, Xia XB. 2015. Petrogenesis of the Early Cretaceous Laguila bimodal intrusive rocks from the Tethyan Himalaya: Implications for the break-up of Eastern Gondwana. Lithos, 236–237, 190–202. doi: 10.1016/j.lithos.2015. 09.00.

Liu ZC, Wang JG, Liu XC, Liu YD, Lai QZ. 2020. Middle Miocene ultrapotassic magmatism in the Himalaya: A response to mantle unrooting process beneath the orogeny. Terra Nova, 33, 240–251. doi: 10.1111/ter.12507.

Lightfoot PC, Hawkesworth CJ, Devey CW, Rogers NW, Van Calsteren WC. 1990. Source and differentiation of Deccan trap lavas: Implications of geochemical and mineral chemical variations. Journal of Petrology, 31(5), 1165–1200. doi: 10.1093/petrology/31.5.1165.

Pearce JA. 2008. Geochemical fingerprinting of oceanic basalts with applications to ophiolite classification and the search for Archean oceanic crust. Lithos, 100(1–4), 1448. doi: 10.1016/j.lithos.2007. 06.016.

Pearce JA. 1982. Trace element characteristics of lavas from destructive plate boundaries. In: Thorpe, R. S. (eds.), Orogenic Andesites. Wiley, Chichester, U. K. , 528–548.

Rudnick RL, Gao S. 2003. The composition of the continental crust. In: Rudnick, R. L. (eds.), The Crust, 1–64.

Shervais JW. 2022. The petrogenesis of modern and ophiolitic lavas reconsidered: Ti-V and Nb-Th. Geoscience Frontiers, 13, 101319. doi: 10.1016/j.gsf.2021.101319.

Shi YR, Hou CY, Anderson JL, Yang TS, Ma YM, Bian WW, Jin JJ. 2018. Zircon SHRIMP U-Pb age of Late Jurassic OIB-type volcanic rocks from the Tethyan Himalaya: Constraints on the initial activity time of the Kerguelen mantle plume. Acta Geochim, 37(3), 441–455. doi: 10.1007/s11631-017-0239-2.

Sciunnach D, Garzanti E. 2012. Subsidence history of the Tethys Himalaya. Earth-Science Reviews, 111(2012), 179–198. doi: 10.1016/j.earscirev.2011.11.007.

Storey BC. 1995. The role of mantle plumes in continental breakup: Case histories from Gondwanaland. Nature 377(6547), 301–308. doi: 10.1038/377301a0.

Sun S, McDonough WF. 1989. Chemical and isotopic systematics of oceanic basalts: Implications for mantle composition and processes, In: Saunders, A. D. and Norry, M. J. (eds.), Magmatism in the ocean basins. Geological Society Special Publication, 42, 313–345.

Wan XQ, Liu WC. 2005. 1∶250000 Gyangze Geological Map. National Geological Archives of China, Beijing

Wang YY, Gao LE, Chen FK, Hou KJ, Wang Q, Zhao LH, Gao JH. 2016. Multiple phases of Cretaceous mafic magmatism in the Gyangze-Kangma area, Tethyan Himalaya, southern Tibet. Acta Petrologica Sinica 32, 3572–3596. (in Chinese with English abstract)

Wang YY, Zeng LS, Asimow P, Gao Li-E, Antoshechkina P, Guo CL, Hou KJ, Tang SH. 2018. Early Cretaceous high-Ti and low-Ti mafic magmatism in Southeastern Tibet: Insights into magmatic evolution of the Comei Large Igneous Province. Lithos, 296–299, 396–411. doi: 10.1016/j.lithos.2017.11.014.

Wang YY, Zeng LS, Zhao LH, Gao Li-E, Gao JH, Hu ZP, Wang HT, Li GX, Di YL, Shen Y, Xu Q. 2020. Baddeleyite and zircon U-Pb ages for of the ultramafic rocks in Chigu Tso area, Southeastern Tibet and their constraints on the timing of Comei Large Igneous Province. China Geology, 2, 262–268. doi: 10.31035/cg2020017.

Wang YY, Zeng LS, Hou KJ, Gao Li-E, Wang Q, Zhao LH, Gao JH, Li GX. 2022. Mantle Source Components and Magmatic Evolution for the Comei Large Igneous Province: Evidence from the Early Cretaceous Niangzhong Mafic Magmatism in Tethyan Himalaya. Journal of Earth Science, 33(1), 133–149. doi: 10.1007/s12583-021-1464-5.

Wei YS, Liang WX, Shang YM, Zhang BS, Pan WY. 2017. Petrogenesis and tectonic implications of about130 Ma diabase dikes in the western Tethyan Himalaya (western Tibet). Journal of Asian Earth Sciences, 143, 236–248. doi: 10.1016/j.jseaes.2017.04.008.

White WM. 2015. Isotopes, DUPAL, LLSVPs, and Anekantavada. Chemical Geology 419, 10–28. doi: org/10.1016/j.chemgeo.2015. 09.026

Wu H, Xu ZY, Yan WB, Hao YJ, Liu HY. 2023. Zircon U-Pb ages and geochemical characteristics of diabase in Nie'erco area, central Tibet: Implication for Neo-Tethyan slab breakoff. Geology in China, 50(6), 1804–1816 (in Chinese with English abstract).

Xia Y, Zhu DC, Wang Q, Zhao ZD, Liu D, Wang LQ, Mo XX. 2014. Picritic porphyrites and associated basalts from the remnant Comei Large Igneous Province in SE Tibet: Records of mantle-plume activity. Terra Nova, 26(6), 487–494. doi: 10.1111/ter.12124.

Xia Y, Wang Q, Zhu DC, Ernst RE, Zhang SQ, Liu D, Zhao ZD. 2020. Intermediate rocks in the Comei large igneous provinces produced by amphibole crystallization of tholeiitic basaltic magma. Lithos, 374–375, 105731. doi: org/10.1016/j.lithos.2020.105731.

Xiao L, Xu YG, Mei HJ, Zheng YF, He B, Pirajno F. 2004. Distinct mantle sources of low-Ti and high-Ti basalts from the western Emeishan large igneous province, SW China: Implications for plume–lithosphere interaction. Earth and Planetary Science Letters 228, 525–546. doi: 10.1016/j.epsl.2004.10.002.

Xu YG, He B, Chung SL, Menzies MA, Frey FA. 2004. Geologic, geochemical, and geophysical consequences of plume involvement in the Emeishan flood-basalt province. Geology 32, 917–920. doi: 10.1130/G20602.1

Zhou Q, Liu Z, Lai Y, Wang GC, Liao ZW, Xu Y, Wu JY, Wang SW, Qing CS. 2017. Petrogenesis of mafic and felsic rocks from the Comei large igneous province, South Tibet: Implications for the initial activity of the Kerguelen plume. Geological Society of America Bulletin, 130, 811–824.

Zhu DC, Chung SL, Mo XX, Zhao ZD, Niu YL, Song B, Yang YH. 2009. The 132 Ma Comei-Bunbury large igneous province: Remnants identified in present-day southeastern Tibet and southwestern Australia. Geology. 37(7), 583–586. doi: 10.1130/ G30001A.1

Zhu DC, Mo XX, Pan GT, Zhao ZD, Dong GC, Shi YR, Liao ZL, Wang LQ, Zhou CY. 2008. Petrogenesis of the earliest Early Cretaceous mafic rocks from the Cona area of the eastern Tethyan Himalaya in south Tibet: Interaction between the incubating Kerguelen plume and the eastern Greater India lithosphere? Lithos, 100 (1–4), 147–173. doi: 10.1016/j.lithos.2007.06.024.